"Handbook of Chemistry and Physics").
(27) Boyer, R. F.; Gillham, J. K. *Org. Coat. Plast. Chem.* **1979**, *41*, 430.
(28) Enns, J. B.; Boyer, R. F. *Org. Coat. Plast. Chem.* **1978**, *38* (1), 387.
(29) Singh, H.; Nolle, A. W. *J. Appl. Phys.* **1959**, *30*, 337.
(30) Williams, G.; Edwards, D. A. *Trans. Faraday Soc.* **1966**, *62*, 1329.
(31) Williams, G.; Watts, D. C. *Trans. Faraday Soc.* **1971**, *67*, 2793.
(32) Boyer, R. F.; Richards-Denny, L.; Elias, H.-G.; Gillham, J. K. *Org. Coat. Plast.* **1980**, *42*, 682.
(33) Simha, R.; Boyer, R. F. *J. Chem. Phys.* **1962**, *37*, 1003. Boyer, R. F.; Simha, R. *J. Polym. Sci., Polym. Lett. Ed.* **1973**, *11*, 33.
(34) Panke, D.; Wunderlich, W. *Proc. 4th ICTA, Budapest* **1974**, *2*, 35–42.
(35) O'Reilly, J. J. *J. Polym. Sci.* **1962**, *57*, 429.
(36) Baer, E.; Kardos, J. L. *J. Polym. Sci., Part A* **1965**, *3*, 2827.
(37) Kijima, T.; Imada, K.; Takayanagi, M. *Rep. Prog. Polym. Phys., Jpn.* **1973**, *16*, 225. These authors note that dT_m/dP tends to increase with T_m.
(38) Frenkel, S.; Baranov, V. G. Institute of Macromolecular Compounds, Leningrad, USSR, personal discussions (Oct 1978).
(39) Frenkel, S.; Baranov, V. G. *Polymer* **1977**, *18*, 228.
(40) Baranov, V. G.; Frenkel, S. *J. Polym. Sci., Part C* **1977**, *61*, 351.
(41) Lobanov, A. M.; Frenkel, S. Ya. *Vysokomol. Soedin.* **1980**, *22*, 1045.

Static and Dynamical Properties of Polystyrene in Carbon Tetrachloride. 1. Characteristic Frequency in the Dilute, Intermediate, and Semidilute Regions†

Y.-H. Lin and B. Chu*

Chemistry Department, State University of New York at Stony Brook, Long Island, New York 11794. *Received March 25, 1980*

ABSTRACT: Dynamical properties, in terms of the characteristic frequency Ω or $1/\tau$, of polystyrene ($\bar{M}_w \sim 1 \times 10^7$) in carbon tetrachloride have been studied from dilute to semidilute polymer concentrations of 0.117 wt % at 18 and 25 °C over a range of scattering angles by means of single-clipped photon correlation of scattered light. In dilute solutions, the dynamical structure factor $S(K,t)$ obeys the form derived by Dubois-Violette and de Gennes, provided that the K range has excluded translational motions of isolated coils as well as fast localized segmental motions. We have also achieved a scaling of Ω/K^2 vs. $Kr_g^{*\dagger}$ by using the Benmouna–Akcasu theory[14] whereby we can determine both the diffusion coefficient and the radius of gyration ($r_g^{*\dagger}$) by making line-width measurements at more accessible scattering angles, e.g., 90°, for high molecular weight polymer samples. We observed a change in Ω, representing an anomalous behavior whose dynamics has not been reported previously. The anomalous phenomenon can be observed only under appropriate conditions but becomes masked for low molecular weight polymers and/or when the probe length (K^{-1}) is inappropriate. It suggests a special property of polymer coils dealing with intermolecular interactions and polymer entanglement.

I. Introduction

In a recent series of articles,[1-6] we reported our studies of static and dynamical properties of polystyrene in *trans*-decalin from around the Θ temperature to about 20 °C above the Θ temperature. We used a low molecular weight polystyrene sample[1-4] ($\bar{M}_w$ = 179 300) in order to avoid observation of Rouse–Zimm motions of polymer coils and examined the changes of osmotic compressibility, diffusion coefficient, and frictional coefficient as a function of temperature and concentration from dilute to concentrated polymer solutions. At finite molecular weight, we observed gradual changes of osmotic compressibility as a function of concentration at various fixed temperatures (20, 30, and 40 °C). Only traces of simple power law relations could be established. By means of a histogram method of data analysis,[7-9] we succeeded in separating the fast pseudogel motions from translational diffusion motions of polymer coils. This pseudogel mode is responsible for the anomalous increase in the variance of the line-width distribution function $G(\Gamma)$ from the dilute to the semidilute region.

By repeating our studies with a high molecular weight polystyrene sample[5,6] ($\bar{M}_w = 1 \times 10^7$), we examined the static and dynamical properties of large polymer coils in the intermediate-K region, where internal motions of polymer segments can play an important role. In dilute solutions, the behavior of the characteristic frequency ($1/\tau$) associated with the dynamical structure factor $S(K,t)$ for an isolated Gaussian coil in the presence of excluded-volume effects has been studied by de Gennes[10] and by Daoud and Jannink.[11] For an unperturbed isolated Gaussian chain in the Zimm limit without excluded-volume effects, Dubois-Violette and de Gennes[12] obtained the characteristic frequency

$$1/\tau = (1/6\pi\sqrt{2})(k_B T/\eta_0)K^3 \quad (1)$$

with a preaveraged Oseen tensor while Akcasu and Gurol[13] obtained a corresponding characteristic frequency

$$\Omega = (1/6\pi)(k_B T/\eta_0)K^3 \quad (2)$$

in the limit of initial decay rate, where $t \to 0$ and k_B, T, and η_0 are the Boltzmann constant, the temperature, and the solvent viscosity, respectively. For small values of K for which $Kr_g \ll 1$, $S(K,t)$ is an exponential function of time with a decay constant $\Gamma = DK^2$, where D is the translational diffusion coefficient and r_g is the radius of gyration of the polymer coil. In the large-K limit for which $Kl \gg 1$, $\Gamma = (k_B T/\xi_0)K^2$, which corresponds to a simple diffusion of segments, with $D_s = k_B T/\xi_0 = k_B T/3\pi\eta_0 l$ and l being the statistical segment length.

In a recent communication, we reported the observation of a dynamical change representing a new anomalous region which occurs before the overlap concentration C^* ($=M/N_A\rho_s r_g^3$, with ρ_s, M, and r_g being the solvent density,

†Work supported by the National Science Foundation Chemistry/Polymer Program (DMR 8016521) and the U.S. Army Research Office.

0024-9297/81/2214-0385$01.25/0

the polymer molecular weight, and the polymer radius of gyration, respectively). Now we wish to show a more detailed analysis of our light scattering line-width and intensity measurements with emphasis on dynamical and static properties of a high molecular weight polystyrene ($\bar{M}_w = 1.3 \times 10^7$) in a marginal solvent (carbon tetrachloride) from dilute solution to the neighborhood of the overlap concentration C^* over a range of temperatures. We shall discuss the line-width results in this article and the static properties from the integrated scattered intensity data in a companion article.

We have discovered that our independent observation of this anomalous behavior may possibly be related to previous reports of the observation of a change in the slope in the heat of mixing[14] and the density[15] of some polymer solutions as a function of concentration. We would like to stress that we made the observation without prior knowledge of the previous reports.[14,15] In fact, Staudinger[16] predicted a possible transition from a discontinuous dilute solution to a continuous solution of pseudonetworks back in 1932. In his Ph.D. thesis, Kotin[17] unsuccessfully attempted to describe the anomalous effects in the heat of mixing, the density, and the viscosity. Our light-scattering measurements in both dynamical and static properties have now permitted us to provide a more detailed picture of this strange behavior of coiling macromolecules in solution. However, in view of the complexity associated with the large number of degrees of freedom of the total polymer segments, our explanation at this time can only be speculative.

II. Brief Theoretical Review

(1) Dilute Solutions. In photon correlation spectroscopy, the net time correlation function $(A\beta)^{1/2}|g^{(1)}(K,t)|$ of scattered electric field for an isolated polymer coil of infinite size with backflow hydrodynamic interactions in a Θ solvent has the form[12]

$$|g^{(1)}(K,t)| \left(\equiv \frac{S(K,t)}{S(K,0)}\right) = \begin{cases} (t/\tau)^{2/3}\int_0^\infty du \exp\{-(t/\tau)^{2/3}u[1 + h(u)]\} & \text{when } t \neq 0 \\ 1 & \text{when } t = 0 \end{cases} \quad (3)$$

where $h(u) = (4/\pi)\int_0^\infty dy\ (\cos y^2/y^3)[1 - \exp(-y^3u^{-3/2})]$ with the inverse of the characteristic time τ defined by eq 1. The quantity $(A\beta)^{1/2}$ represents the numerical value of the unnormalized net time correlation function at $t = 0$. Equation 3 is valid in the intermediate-K region (where $Kr_g \gg 1$ and $Kl \ll 1$) for a single coil of infinite size and is referred to as the DD theory. However, in the absence of any theory for the entire correlation function applicable at finite concentrations in fair (and good) solvents, we have used the DD theory to analyze our data in dilute solutions of polystyrene/CCl_4. Furthermore, we expect that eq 3 should describe the dynamics of large polymer coils even in fair solvents as long as the polymer chain remains a Gaussian coil. This argument can be supported from eq 12 of ref 12, which indicates that only small values of s in the integral contribute toward the Rouse–Zimm relaxation modes. In terms of the blob theory, there is a cutoff distance s_τ beyond which the excluded-volume effect is important. Therefore, eq 3 holds so long as s_τ remains sufficiently large that the upper limit of the integral in eq 12 of ref 12 can be replaced by s_τ without appreciable errors.

Benmouna and Akcasu[18] introduced a characteristic frequency Ω as the initial slope of log $S(K,t)$, i.e.

$$\Omega = -\lim_{t\to 0} \mathrm{d}[\log S(K,t)]/\mathrm{d}t \quad (4)$$

which shows that Ω can be determined precisely from the measured short-time behavior of log $S(K,t)$ or from the large-frequency (ω) behavior of $S(K,\omega)$, provided that these limits are experimentally accessible. Following Farnoux[19] and Daoud et al.[11,20] and with the preaveraged Oseen tensor, Benmouna and Akcasu obtained (the BA theory) for a single chain

$$\Omega(K,t) = \frac{K^2}{\beta\xi_0}\left\{1 + A_1\left[\left(\gamma\left(\frac{1-\nu}{2\nu}, a_2\right) - \gamma\left(\frac{1-\nu}{2\nu}, a_1\right)\right) - \frac{Z}{a_1^{1/2\nu}}\left(\gamma\left(\frac{2-\nu}{2\nu}, a_2\right) - \gamma\left(\frac{2-\nu}{2\nu}, a_1\right)\right)\right] + A_2\int_{N_\tau^{-1/2}}^1 du\ (1 - Zu^2)e^{-a_1u^2}\right\} \times \left\{1 + \frac{N_\tau}{\nu a_1^{1/2\nu}}\left[\left(\gamma\left(\frac{1}{2\nu}, a_2\right) - \gamma\left(\frac{1}{2\nu}, a_1\right)\right) - \frac{Z}{a_1^{1/2\nu}}\left(\gamma\left(\frac{1}{\nu}, a_2\right) - \gamma\left(\frac{1}{\nu}, a_1\right)\right)\right] + \frac{2N_\tau}{a_1}(e^{-a_1/N_\tau} - e^{-a_1}) + \frac{2N_\tau^2}{Na_1}\left(e^{-a_1} + \frac{e^{-a_1}}{a_1} - \frac{e^{a_1/N_\tau}}{N_\tau} - \frac{e^{-a_1/N_\tau}}{a_1}\right)\right\}^{-1} \quad (5)$$

where $\bar{A}_1 = BN_\tau^{1/2}/2\nu a_1^{(1-\nu)/2\nu}$, $B = [2/(6\pi)^{1/2}\pi](\xi_0/\eta_0 l)$, $A_2 = 2BN_\tau^{1/2}$, $a_1 = K^2\xi_\tau^2/6$, $a_2 = a_1/Z^{2\nu}$, $Z = N_\tau/N$, ξ_τ $(=lN_\tau^{0.5})$ is a measure of distance beyond which the excluded-volume interaction between monomers becomes important, and $\gamma(\nu,x)$ is the incomplete γ function. The quantity $\xi_0/\eta_0 l$ suggests a measure of the relative strength of the hydrodynamic interactions. With $D_s = k_BT/3\pi\eta_0 l$, $\xi_0 = 3\pi\eta_0 l$ corresponds to a Stokes relationship for beads of hard spheres of radius $l/2$. In the intermediate-K range, where $Kl \ll 1$, eq 3 implicitly assumes that the exact value of $\xi_0/\eta_0 l$ is not important.

(2) Semidilute Solutions. In the semidilute region ($C > C^*$) the average distance ξ between entanglement points is independent of molecular weight.[21] If we take the correlation length ξ to be of the same order as r_g and the crossover concentration C^* to be proportional to Mr_g^{-3}, where M is the molecular weight of the polymer, then

$$\xi \propto r_g(C/C^*)^q \quad (6)$$

with $q = \nu/(1 - 3\nu)$. Experimentally, the relation $q = \nu/(1 - 3\nu)$ does not hold for most polymers of finite molecular weight. For $K\xi \gg 1$, the measured time correlation reflects dynamical properties of the polymer chain or distances shorter than ξ whereby eq 1 and 2 represent the characteristic frequencies with a K^3 dependence. For $K\xi \ll 1$, the line width Ω has the form

$$\Omega = D_cK^2 \quad (7)$$

where D_c is an effective mutual diffusion coefficient.

III. Experimental Methods

(1) Sample Preparations. Polystyrene was purchased from Toyo Soda Manufacturing Co. Ltd., Japan, TSK Standard F-1500. We used the same sample as that reported previously.[5,6] Reagent grade carbon tetrachloride was filtered through a Millipore filter of nominal pore diameter 0.22 μm. We first made a 0.328 wt % polystyrene solution in CCl_4. It was centrifuged at 6000g (gravitational acceleration) for 8 h. Then, we took the middle portion of the centrifuged solution as our stock solution. The condition for the centrifugation was determined in the same manner as

Table I
Parameters and Ranges of the Cumulant Function $F(t/\tau)$

$F(x) = a\exp(bx + cx^2 + dx^3 + ex^4 + fx^5 + gx^6)$ with $x = t/\tau$

	$R = S(x)/S(0)$			
	$R > 0.808$	$0.808 > R > 0.509$	$0.509 > R > 0.122$	$0.122 > R > 0.051$
a	0.981 176 081	0.962 238 061	0.964 823 117	0.905 503 319
b	−4.005 609	−2.618 011 4	−2.546 629 3	−2.272 559 2
c	4.228 31 × 10	2.450 96	8.026 39 × 10^{-1}	2.990 53 × 10^{-1}
d	−5.831 05 × 10^2	−1.218 67 × 10	−5.428 99 × 10^{-1}	−1.460 48 × 10^{-2}
e	4.050 59 × 10^3	3.685 34 × 10	3.368 35 × 10^{-1}	−2.484 25 × 10^{-2}
f	−1.047 35 × 10^4	−4.824 86 × 10	−1.548 91 × 10^{-1}	8.359 04 × 10^{-3}
g	−5.219 79 × 10^3	1.538 41 × 10	3.609 51 × 10^{-2}	−7.784 32 × 10^{-4}

discussed previously.[5] Solutions at lower concentrations were prepared by dilution of a known amount of the centrifuged stock solution directly in the light scattering cell, using filtered CCl_4. In order to minimize evaporation losses, the precision-bore cylindrical light scattering cell containing known amounts of CCl_4 and the stock solution was quickly frozen in liquid nitrogen before the cell tip was flame-sealed.

(2) Apparatus and Method of Data Analysis. We used the same light scattering spectrometer which has been described in detail elsewhere.[22,23] In the present experiment, we used a Spectra Physics Model 165 argon ion laser operating at 488.0 nm and ~200 mW and a 96-channel single-clipped photon correlator. Temperature was controlled and measured to ±0.01 °C. Other details can be found in our previous studies.[1-6]

The measured single-clipped photocount autocorrelation function has the form

$$G_k^{(2)}(t) = A(1 + \beta|g^{(1)}(t)|^2) \quad (8)$$

where k, A, and β are the clipping level, the background, and an unknown parameter in the data-fitting procedure. The net signal correlation function $A\beta|g^{(1)}(t)|^2$ is then fitted according to eq 3, using $1/\tau$ and $A\beta$ as the two unknown parameters by the method of least-squares.

The least-squares fitting procedure is as follows.

Numerical values of the correlation function $[S(K,t)/S(K,0)]^2$ were generated from eq 3 as a function of reduced time t/τ. The generated correlation function was then least-squares fitted by a sixth-order cumulant function covering a limited range of the reduced delay time. We used four cumulant functions $F(t/\tau)$ to represent the theoretical $[S(K,t/\tau)/S(K,0)]^2$. The parameters and ranges of $F(t/\tau)$ are listed in Table I. The measured time correlation was then least-squares fitted to $F(t/\tau)$.

IV. Results and Discussion

We shall present our results in the dilute-solution region ($C \ll C^*$) based on an analysis of $(A\beta)^{1/2}|g^{(1)}(\tau)|$ in terms of (1) the DD theory and (2) the BA theory. We then extend our analysis in (3) the intermediate region before we reach (4) the semidilute region ($C \gtrsim C^*$).

(1) Analysis in Terms of the DD Theory. The DD theory assumes isolated polymer coils of infinite size. With a high molecular weight ($\bar{M}_w = 1 \times 10^7$) polystyrene sample dissolved in a fair solvent (carbon tetrachloride), we are in the neighborhood of the intermediate-K range ($Kr_g \gg 1$ and $Kl \ll 1$). Figure 1 shows deviation plots of a dilute solution of 0.0113 wt % polystyrene in carbon tetrachloride measured at $\theta = 30$, 45, 75, and 135°. At $\theta = 30$, $K = 9.786 \times 10^4$ cm^{-1}, and $Kr_g = 2.32$, the measured time correlation function $(A\beta)^{1/2}|g_m^{(1)}(\tau)|$ still contains some characteristics of the slower translational diffusive motion. Therefore, eq 3 is not an excellent representation of the polymer dynamics occurring in a fairly dilute solution. At $\theta = 45$ and $Kr_g = 3.43$, the deviation plot, as shown in Figure 1b, between theory and experiment agrees to within experimental error limits over several characteristic decay times. The agreement between eq 3 and the measured time correlation function deteriorates as Kr_g increases from $\theta = 75°$ to $\theta = 135°$ because at $\theta = 135°$, $K = 3.493 \times 10^5$ cm^{-1}, $Kr_g = 8.28$, and $Kl = 0.139$. There, we begin to observe the faster localized segmental diffusive motions which could be responsible for the poor agreement especially over the shorter decay time ranges, as shown in Figure 1d. As we increase the concentration, the deviation between eq 3 and the measured time correlation function again increases. Figures 2 and 3 show plots of the measured time correlation function $A\beta|g_m^{(1)}(\tau)|^2$ (dots) and the computed $A\beta|g^{(1)}(\tau)|^2$ (solid line) as well as percent deviation vs. the delay channel number. The percent deviation plots clearly indicate that eq 3 can no longer represent $|g_m^{(1)}(\tau)|$ even in its functional form, as the shape of the deviation curve in Figures 2 and 3 remains essentially the same. At finite concentrations, we do not expect eq 3 to hold. However, we continue to use the DD theory for our experimental data even though eq 3 predicts an incorrectly shaped function. In this sense, identification of a *single* characteristic frequency is not strictly correct. Nevertheless, we believe that $1/\tau$ represents the main frequency contribution for an unperturbed Gaussian chain in the Zimm limit with a preaveraged Oseen tensor. Deviations of the $1/\tau$ value from eq 1 at finite concentrations can be considered as contributions first due to interactions between neighboring polymer coils and then due to partial overlaps of polymer coils at $C \to C^*$. Figures 4 and 5 show plots of log $(1/\tau K^2)$ vs. concentration at 18 and 25 °C, respectively. At $\theta = 135°$, the extrapolated values of $1/\tau K^2$ at infinite dilution coincide with the theoretical values computed from eq 1 using known values of η_0, K, and T.

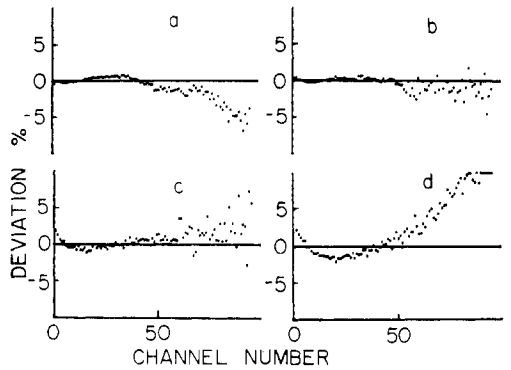

Figure 1. Plots of percent deviation as a function of delay channel number. The y axis represents % dev = $100(|g_m^{(1)}(\tau)|^2 - |g^{(1)}(\tau)|^2)/|g^{(1)}(\tau)|^2$. $|g^{(1)}(\tau)|^2$ denotes the computed value based on eq 3 and the subscript m denotes the measured value. The x axis represents the delay channel number. $C = 0.0113$ wt % polystyrene in CCl_4.

	θ, deg	$\Delta\tau$, μs	$10^2(1/\tau)$, s^{-1}	Kr_g	t, °C
a	30	75	2.51	2.324	18
b	45	35	6.43	3.979	18
c	75	8	22.4	5.467	18
d	135	2.4	69.7	8.296	18

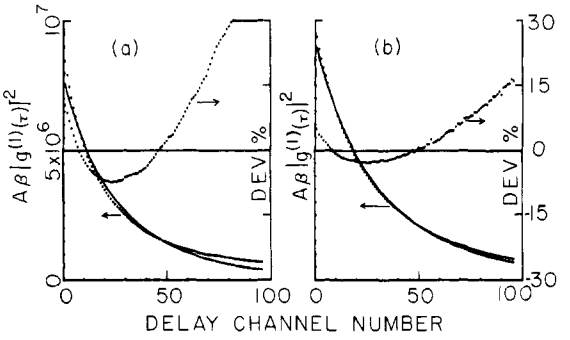

Figure 2. Plots of $A\beta|g_m^{(1)}(\tau)|^2$ (dots) and $A\beta|g^{(1)}(\tau)|^2$ (solid line) as a function of delay channel number. The y axis on the left-hand side represents arbitrary intensity units. The y axis on the right-hand side represents percent deviation as defined in Figure 1. C = 0.0316 wt % polystyrene in CCl_4.

$$C_1^* = M/N_A\rho_s(^4/_3\pi r_g^3) = 0.0241 \text{ wt \%}$$

	θ, deg	Δτ, μs	$10^2(1/\tau)$, s^{-1}	Kr_g	t, °C
a	30	150	1.07	2.324	18
b	135	2.2	62.09	8.296	18

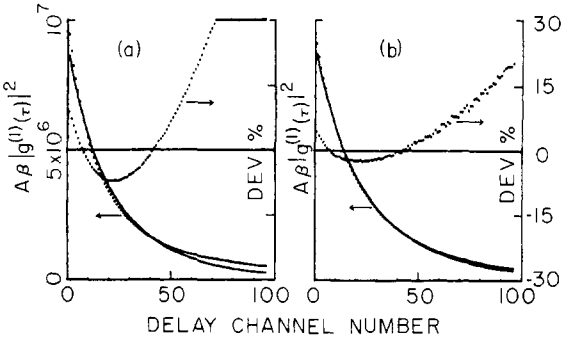

Figure 3. Plots of $A\beta|g_m^{(1)}(\tau)|^2$ (dots), $A\beta|g^{(1)}(\tau)|^2$ (solid line), and percent deviation vs. delay channel number. The notations are defined in Figures 1 and 2. C = 0.0446 wt % polystyrene in CCl_4.

$$C_1^* = 0.0241 \text{ wt \%}$$

	θ, deg	Δτ, μs	$10^2(1/\tau)$, s^{-1}	Kr_g	t, °C
a	30	125	1.59	2.324	18
b	135	2.7	65.02	8.296	18

As the DD theory is valid for a single polymer coil of infinite size, the large Kr_g value of about 8.3 at θ = 135° signifies that the dynamical behavior expressed in terms of $1/\tau$ has already reached the asymptotic K^3 region. The interesting aspect of this agreement between experiment and theory is that eq 1 is based on a preaveraged Oseen tensor. Therefore, we need to be concerned with more fundamental aspects on the assumptions of the Rouse–Zimm model which has been taken for granted so far. Figure 4 shows results of our previous communication at θ = 45 and 135°. The additional measurements at θ = 30 and 75° and those shown in Figure 5 at 25 °C confirm our conclusion that eq 1 is a good representation of experimental facts at infinite dilution, provided that the asymptotic K^3 region has been reached.

At finite concentrations, the $1/\tau$ value goes through a maximum and then a minimum with increasing concentration, as shown in Figures 4 and 5. By arbitrarily de-

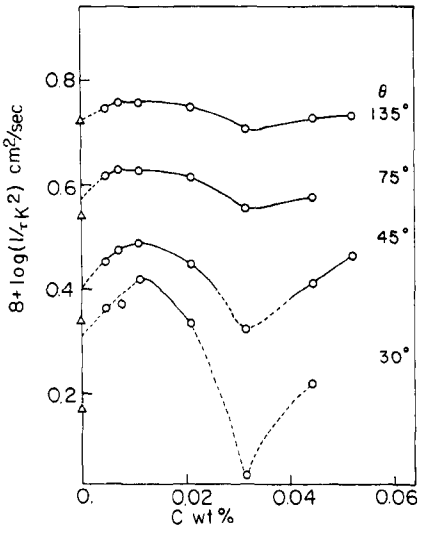

Figure 4. Plots of log $(1/\tau K^2)$ vs. concentration (wt %) at scattering angles θ = 30, 45, 75, and 135° and at 18 °C. The hollow triangles represent computed values of log $(1/\tau K^2)$ from eq 1, using known values of η_0, K, and T.

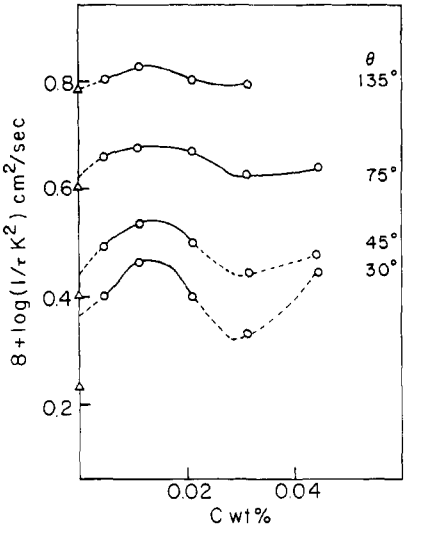

Figure 5. Plots of log $(1/\tau K^2)$ vs. concentration (wt %) at scattering angles θ = 30, 45, 75, and 135° and at 25 °C. The hollow triangles represent computed values of log $(1/\tau K^2)$ from eq 1, using known values of η_0, K, and T.

fining an overlap concentration C_1^* $[=M/N_A\rho_s(^4/_3\pi r_g^3)]$ which is approximately $C^*/4$, we have noted that the polymer chain dynamics goes through an anomalous region. Near C_1^*, the RSQ value in a least-squares fitting of $|g_m^{(1)}(\tau)|$ with eq 3 decreases dramatically, where

$$\text{RSQ} = 1 - \sum_i^N (Y_i - Z_i)^2 / [\sum_i^N Y_i^2 - (\sum_i^N Y_i)^2/(N+1)] \quad (9)$$

with $Z_i \equiv |g^{(1)}(\tau)|^2$ of eq 3 and $Y_i \equiv |g_m^{(1)}(\tau)|^2$. Figure 6 shows typical plots of RSQ as a function of concentration at 18 °C and θ = 30, 45, 75, and 135°. At concentrations slightly greater than C_1^*, the RSQ value clearly indicates that the dynamics becomes complex and eq 3 is no longer a good representation of experimental facts.

In a fair solvent and at *low* concentrations (C < 0.015 wt %) the characteristic frequency $(1/\tau)$ increases with

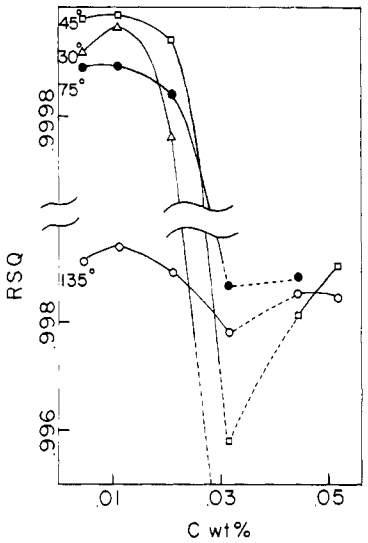

Figure 6. Plots of RSQ vs. concentration (wt %) at scattering angles θ = 30, 45, 75, 135° and at 18 °C.

concentration as expected. Equation 3 represents the time behavior of $|g_m^{(1)}(\tau)|$ fairly well as the RSQ values are in the 0.9999 range at θ = 30, 45, and 75°. At θ = 135°, we believe that the presence of the faster localized segmental diffusive motions may be responsible for the decrease in RSQ value as shown by the relatively poorer fitting in Figure 1d. The more interesting behavior in the $1/\tau K^2$ vs. C plots is the wiggle of the characteristic frequency as shown in Figures 4 and 5. This yet unexplained behavior near C_1* becomes more prominent at smaller scattering angles and at lower temperatures. Near C_1*, we have observed some overlap of the polymer coils as in the case of polystyrene in *trans*-decalin.[4] The solution, however, has not yet reached the semidilute region. Consequently, we attribute the anomaly as due to significant intermolecular interactions between polymer coils. The effect is absent in the polystyrene–*trans*-decalin system[1-6] for both a low molecular weight ($\bar{M}_w \sim 1.8 \times 10^5$) and a high molecular weight ($\bar{M}_w \sim 1.2 \times 10^7$) sample.

In the absence of a quantitative theory, we can suggest only a physical picture of the polymer solution at concentrations near C_1*. In very dilute solutions, we visualize each individual polymer molecule as an isolated entity in a relatively homogeneous sea of solvent molecules, while in the semidilute region, the polymer coils are entangled with many overlapping points whose concentration increases with polymer concentrations and whose distribution is relatively uniform throughout the solution. The intermediate concentration behavior from dilute solution to the semidilute solution appears when polymer coils are relatively close to one another. Furthermore, the dynamics must become more complex as additional characteristic times related to polymer coil interpenetration could be present. Consequently, eq 3 becomes a poorer representation of the measured time correlation function, as shown in Figures 2, 3, and 6. It is important to note that this anomalous behavior is observed only when the K range is compatible with the polymer coil dimension and penetration characteristics. The anomalous concentration dependence of $1/\tau$ in the intermediate concentration region is further confirmed by similar behavior in the static properties, such as the osmotic compressibility, which will be discussed in a companion article of this series.

(2) Analysis in Terms of the BA Theory. In the BA theory,[18a] the initial slope $\Omega(K)$, as expressed in eq 4, is calculable for all values of K as a function of temperature,

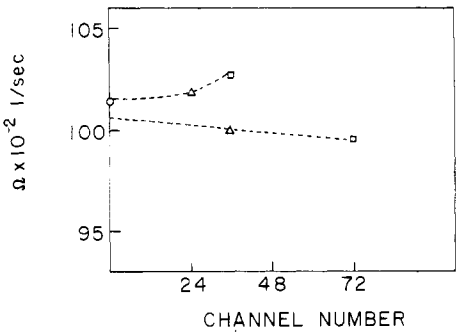

Figure 7. Plots of $\bar{\Gamma}$ ($\equiv\Omega$) values based on fourth-order (□) and third-order cumulant fits (△) vs. number of delay channels. The hollow circle represents a second-order extrapolation of Ω to $t \rightarrow 0$; C = 0.0048 wt % at 18 °C; $\Delta\tau$ = 2.5 μs; θ = 135°.

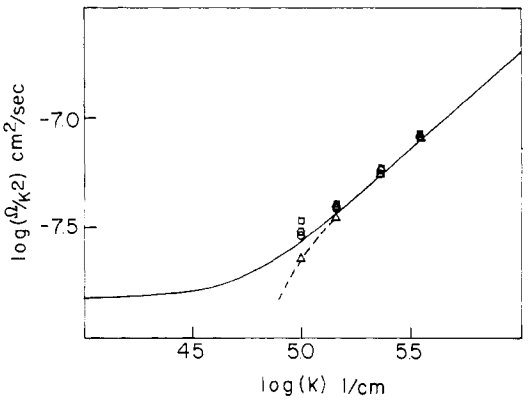

Figure 8. log–log plots of Ω/K^2 vs. K at concentrations 0.0048 (○), 0.00734 (○), 0.0113 (□), and 0.0316 (△) wt %. The solid line represents the computed curve based on eq 5 and has been allowed to scale along the vertical axis.

in terms of the "blob" theory of chain statistics.[20] The practical difficulty with this method is that the initial slope is hard to measure in the intermediate-K range. Akcasu et al. have discussed the details elsewhere.[24] We used two different modified approaches to determine the initial decay rate $\Omega(K)$

(a) First, we used a single-exponential function to force fit $|g_m^{(1)}(t)|$ over a range of decreasing delay channel numbers. The Ω value extrapolated to zero delay time for a typical sample is shown as a hollow circle in Figure 7.

(b) Different order cumulants[26] are used in the fitting procedure. The extrapolation is based on the fact that different order cumulants are required to fit the time correlation function, depending upon the range of delay times used.[27] The correct $\bar{\Gamma}$ value can be extracted by using experimental ranges of delay times with appropriate numbers of cumulants, as shown in Figure 7.

Plots of log (Ω/K^2) vs. log K at concentrations 0.0048, 0.00734, and 0.0113 wt % are shown in Figure 8. The solid line represents the theoretical curve using eq 5 with N/N_τ = 1076, N_τ = 5.8, l = 39.7 Å, and $\xi_0/\eta_0 l = 3\pi$. These values were based on an estimate of αn (=4) by Akcasu and Han[28] for polystyrene in different solvents and the results of the static properties of these samples (next article).

At finite concentrations, the data points deviate from the theoretical K dependence of $\Omega(K)/K^2$ (eq 5). There may be at least two reasons responsible for this deviation. Firstly, Akcasu and Benmouna[18b] introduced a concentration-dependent cutoff parameter N_C which characterizes the extent of the screening of the intramolecular excluded-volume effect due to neighboring polymer coils. Secondly, at finite concentrations, the static and dynamical

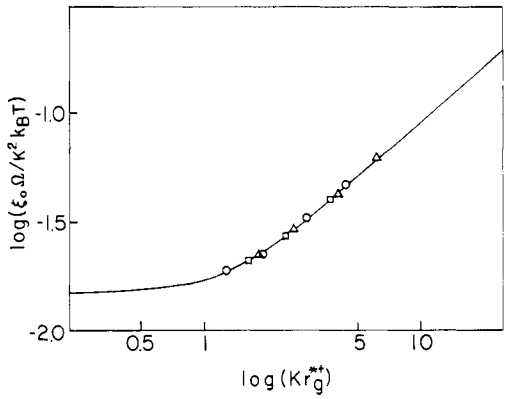

Figure 9. Results of least-squares fitting to the theoretical curve of Figure 8 by allowing the experimental data for each concentration to scale along both log (Ω/K^2) and log $(Kr_g{}^{*\dagger})$. C = 0.0048 (△), 0.00734 (□), and 0.0113 (○) wt %. $r_g{}^{*\dagger}$ is the apparent radius of gyration based on fitting of Ω/K^2 to the BA theory.

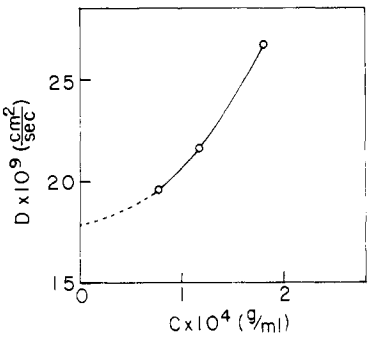

Figure 10. Plot of D vs. concentration. $D_0 \approx (1.79 \pm 0.12) \times 10^{-8}$ cm^2/s.

pair correlation between segments of different polymer molecules is present in the general form of $\Omega(K,C)$

$$\Omega(K,C) = \mathbf{KK}:\sum_{m,n}[\langle D_{1m,1n}e^{i\mathbf{K}\cdot(\mathbf{R}_{1n}-\mathbf{R}_{1m})}\rangle + (n_p - 1) \times \langle D_{1m,2n}e^{i\mathbf{K}\cdot(\mathbf{R}_{2n}-\mathbf{R}_{1m})}\rangle]/\sum_{m,n}[\langle e^{i\mathbf{K}\cdot(\mathbf{R}_{1n}-\mathbf{R}_{1m})}\rangle + (n_p - 1)\langle e^{i\mathbf{K}\cdot(\mathbf{R}_{2n}-\mathbf{R}_{1m})}\rangle] \quad (10)$$

where n_p is the number of polymer chains in the scattering volume. $\Omega(K,C)$ depends on concentration. In practice, we take Ω/K^2 as a function of $Kr_g{}^{*\dagger}$, where $r_g{}^{*\dagger}$ is now an apparent radius of gyration at some low finite concentrations. We can then scale the log–log plot of Ω/K^2 vs. K along both axes of Figure 8. By using $r_g{}^{*\dagger}$ as an additional variable and by forcing the experimental data onto the theoretical curve of Figure 8, which is being used as a master curve, we then get the apparent $r_g{}^{*\dagger}$ value to be 1.79 × 10^3, 1.64 × 10^3, and 1.29 × 10^3 Å at C = 0.0048, 0.00734, and 0.0113 wt %, respectively. Figure 9 shows a log–log plot of Ω/K^2 vs. $Kr_g{}^{*\dagger}$. The solid line is based on the theoretical curve of Figure 8. These $r_g{}^{*\dagger}$ values are in very good agreement with the results of the z-average radius of gyration $\langle r_g{}^2\rangle_z{}^{*1/2}$, as defined by eq 12 in the companion paper, from intensity measurements of the same samples, where $\langle r_g{}^2\rangle_z{}^{*1/2}$ = 1.80 × 10^3, 1.54 × 10^3, and 1.24 × 10^3 Å at the corresponding concentrations. The excellent fit between experimental data and the theoretical curve, together with the resulting agreement in the apparent radius of gyration and $\langle r_g{}^2\rangle_z{}^{*1/2}$, suggests that the shape of the theoretical curve in a log (Ω/K^2) vs. log $(Kr_g{}^{*\dagger})$ plot is relatively insensitive to concentration changes at finite low concentrations.

By following the theoretical curve of Figure 9, we can now compute the asymptotic diffusion coefficient D in the limit $Kr_g \ll 1$ at finite low concentrations because we can obtain the Ω/K^2 value from known values of $Kr_g{}^{*\dagger}$ by using the theoretical curve in Figure 9. Figure 10 shows a plot of the diffusion coefficient as a function of concentration for the three samples at finite low concentrations. The extrapolated value at infinite dilution D_0 can be estimated to be 1.79 × 10^{-8} cm^2/s. By the Stokes–Einstein relation, we get the hydrodynamic radius $r_h = k_BT/6\pi\eta_0D_0$ = 1.19 × 10^3 Å. The hydrodynamic radius for the same polystyrene sample in *trans*-decalin at Θ temperature was found to be 760 Å. If we take r_h in each Θ solvent to be the same at its Θ temperature, we can calculate an expansion coefficient $\alpha_h = r_h/r_{h,\Theta}$ = 1.56. In terms of the blob model, BA have derived α_h as a function of N/N_τ. The theoretical result has been used by Akcasu and Han[28] for comparison over a wide range of experimental data of polystyrene of different molecular weights in a variety of solvents. In our previous work, we have found very good agreement between the BA theory and our experiments on the polystyrene ($\bar{M}_w$ = 1.2 × 10^7)–*trans*-decalin system.[5,6] The result of the present study is denoted by a filled square in Figure 11 and is in very good agreement with the theoretical prediction.

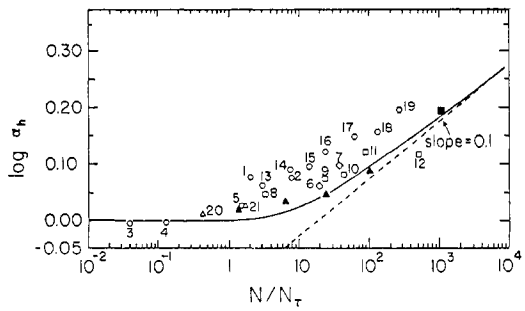

Figure 11. Plots of log α_h vs. log (N/N_τ): (■) present study; (▲) data reported by Nose and Chu;[5] solid line, the BA theory; other hollow symbols, see ref 22.

Table II
Ratio of $\Omega/(1/\tau)$ for Polystyrene/CCl_4 at Dilute Finite Concentrations and 18 °C

	θ, deg			
concn, wt %	30	45	75	135
0.0048	1.26	1.36	1.36	1.49
0.0113	1.31	1.31	1.41	1.50

As the condition $Kr_g \ll 1$ is difficult to achieve in light scattering studies of very large polymer molecules, the translational diffusion coefficient can be measured only at (fairly inaccessible) small scattering angles. Furthermore, as $\Omega = DK^2$ when $Kr_g \ll 1$, the narrow line widths at small K values require long measurement times. Consequently, it has been difficult to test the BA theory by using very high molecular weight polymer samples dissolved in fairly good solvents. We have shown one approach whereby we can obtain diffusion coefficients at low but finite concentrations by extrapolating the characteristic frequencies measured at more accessible scattering angles, where $Kr_g \gtrsim 1$, through the theoretical $Kr_g{}^{*\dagger}$ dependence of Ω/K^2, to the limit $Kr_g{}^{*\dagger} \to 0$.

(3) Comparison of Analyses in Terms of the DD and the BA Theories. The characteristic relaxation rates $1/\tau$ and Ω as determined from fitting the measured time correlation function to eq 3 and by extracting the initial slope of log $S(K,t)$ (eq 4), respectively, are expected to have a constant scaling ratio in the appropriate K range. The values of the ratio of $\Omega/(1/\tau)$ for solutions of 0.0048 and 0.0113 wt % at 18 °C and different scattering angles are listed in Table II.

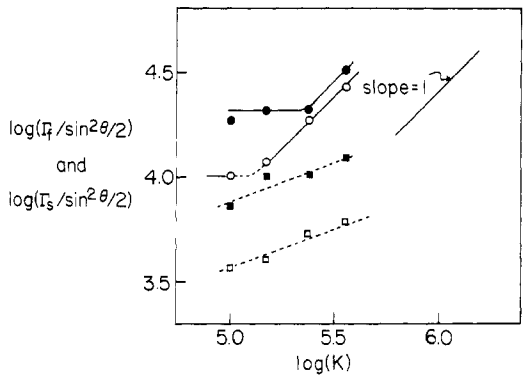

Figure 12. log–log plots of $\Gamma_f/\sin^2(\theta/2)$ and $\Gamma_s/\sin^2(\theta/2)$ as a function of K. Fast mode: (●) C = 0.117 wt %; (○) C = 0.0731 wt %. Slow mode: (■) C = 0.0117 wt %; (□) C = 0.0731 wt %.

In a Θ solvent and according to eq 1 and 2, the ratio $\Omega/(1/\tau)$ is 1.414 (=$\sqrt{2}$), which is compared very favorably with the values listed in Table II, especially when $\theta = 75°$, where the K^3 dependence of eq 1 and 2 holds well. At the scattering angle $\theta = 135°$, the $\Omega(t\rightarrow 0)$ value may contain contributions of fast, more localized segmental motions and this may lead to a larger value of $\Omega/(1/\tau)$ than 1.414.

(4) Intermediate Region. In the intermediate region ($C \sim C_1^*$), we have observed a dramatic change of Ω/K^2 values, especially at scattering angles below 45°, as shown in Figure 8. In the K region corresponding to $\theta \approx 30°$, $\Omega(K)$ has approached a K^4 limit. For a single labeled chain in the presence of other invisible chains, Akcasu and Benmouna[14] have indicated that the screening of intramolecular hydrodynamic interaction between segments by neighboring polymer molecules leads to a K^4 scaling of $\Gamma(K)$. In the intermediate region ($C \sim C_1^*$), there is not yet any clear appearance of entanglement points among polymer chains. Thus, the anomalous change in the characteristic frequency Ω may possibly be related to the mutual interpenetration of polymer coils and the mutual screening of hydrodynamic interactions. At concentrations beyond the intermediate region, $C > C_1^*$, entanglements among polymer coils become appreciable.[1-6] Thus, the anomalous behavior in the characteristic frequency leads us to suggest that the polymer coil in the intermediate concentration region may be visualized as having metastable states depending upon previous thermodynamic history.

(5) Semidilute Region. At concentrations 0.0731 and 0.117 wt % ($C > C_1^*$), we are able to distinguish two modes of motions, in agreement with our previous findings on the polystyrene ($\bar{M}_w = 1.3 \times 10^7$)–*trans*-decalin system.[1-6] The measured time correlation function was analyzed by using the approximate equation

$$(A\beta)^{1/2}|g^{(1)}(K,t)| = A_s e^{-\Gamma_s t} + A_f e^{-\Gamma_f t + \mu_2 t^2} \qquad (11)$$

where the subscripts s and f denote the slow and the fast mode. μ_2/Γ_f^2 is the variance related to the line-width distribution of the fast mode. The results of our analysis are shown in Figure 12. The fast-decay mode Γ_f has a K^3 dependence for θ above 37° at C = 0.0731 wt % and for θ above 75° at C = 0.117 wt %. According to eq 2 and 7, we expect to observe a transition from the K^2 to the K^3 dependence as $K\xi$ is varied from much less than 1 to much greater than 1. It is surprising to find that the transition is rather sharp. We shall take advantage of this observation and utilize the changeover position as an estimate of the correlation length ξ between adjacent entanglement points. At the changeover point, $\xi \approx 1/K$. Thus we obtained ξ = 840 and 435 Å at C = 0.0731 and 0.117 wt %, respectively. These values are indeed related to the corresponding apparent r_g^* values of 677 and 345 Å from light scattering intensity measurements. At each fixed concentration, the ratio of ξ to the apparent r_g^* is about 1.25 (840–677 = 1.24 and 435/345 = 1.26), indicating the same order of magnitude. The apparent r_g^* (or more precisely, the apparent characteristic length) from intensity measurements is smaller than ξ partly because we have not excluded entanglement effects in our intensity data analysis.[4] The agreement, however, is qualitative. In our present study, we have observed a pseudotransition region $C^* > C \gtrsim C_1^* \approx C^*/4$, where polymer coils can interpenetrate without appreciable entanglement. At higher concentrations, ξ is much smaller than r_g. Thus, the relation $\xi \sim r_g$ no longer holds and we do not expect the relation $q = \nu/(1 - 3\nu)$ in eq 6 to hold. For ν = 0.6, q = 0.75. If we take the transition-point values of K^* ($\approx 1/\xi$) from plots of $1/\tau K^2$ vs. K at different concentrations, we can estimate an apparent q value of −1.5, which is quite different from −0.75 of eq 12. The slow-mode Γ_s has a $K^{2.4}$ dependence. We have no explanation except for the fact that we used an approximate expression (eq 11) in our analysis and believe that the value should not be taken seriously.

V. Conclusions

The DD theory based on a single chain of infinite size at Θ condition provides an excellent expression for $S(K,t)$ in dilute solutions of polystyrene (coiling polymer) in carbon tetrachloride (a fair solvent), provided that measurements are carried out at the appropriate K range where translational motions of entire individual molecules or localized segmental diffusive motions are absent. The $1/\tau$ values at infinite dilution agree with the prediction of eq 1 for $Kr_g \gg 1$. Therefore, the approximations of the Rouse–Zimm model must include canceling effects. We have observed an anomalous phenomenon which occurs in the neighborhood of C_1^*, where polymer coils tend to interpenetrate before appreciable entanglements take place. In the intermediate concentration region, eq 3 is no longer a good representation of $S(K,t)$ and the change in $1/\tau$ is quite dramatic in the appropriate K range, as shown by Figures 4 and 5 at $\theta = 30°$. The effect is nonexistent for the same polymer in *trans*-decalin.[5,6]

The BA theory[18a] provides an excellent expression for the Ω as a function of K and r_g. We have succeeded in scaling Ω/K^2 as a function of $Kr_g^{*\dagger}$, as shown in Figure 9 Consequently, we can determine the translational diffusion coefficient and the radius of gyration at finite concentrations in the dilute solution region by making line-width measurements where eq 7 is not valid.

Our empirical procedure of using a concentration-dependent characteristic frequency $1/\tau$ and an effective radius of gyration ($r_g^{*\dagger}(C)$) assumes that the theoretical forms of $S(K,t)$ (eq 3) and $\Omega(K,t)$ (eq 5) for a single chain can be used to analyze experimental data at finite concentrations. This approach is very similar to that invoked by Muthukumar and Freed.[25] The very good agreement of the $r_g^{*\dagger}$ values with the results of the z-averaged radius of gyration $\langle r_g^2\rangle_z^{*1/2}$ (eq 12 of paper 2) and the result shown in Figure 1b suggest that eq 3 and 5 are not sensitive to concentration so long as effective parameters are used.

In the semidilute region, $1/\tau$ increases as a function of concentration. The essential behavior is similar to those reported elsewhere.[6]

References and Notes

(1) Chu, B.; Nose, T. *Macromolecules* **1979**, *12*, 347.
(2) Nose, T.; Chu, B. *J. Chem. Phys.* **1979**, *70*, 5332.

(3) Nose, T.; Chu, B. *Macromolecules* **1979**, *12*, 590.
(4) Chu, B.; Nose, T. *Macromolecules* **1979**, *12*, 599.
(5) Nose, T.; Chu, B. *Macromolecules* **1979**, *12*, 1122.
(6) Chu, B.; Nose, T. *Macromolecules* **1980**, *13*, 122.
(7) Chu, B.; Gulari, Esin; Gulari, Erdogan *Phys. Scr.* **1979**, *19*, 476.
(8) Gulari, Esin; Gulari, Erdogan; Tsunashima, Y.; Chu, B. *J. Chem. Phys.* **1979**, *70*, 3965.
(9) Gulari, Erdogan; Gulari, Esin; Tsunashima, Y.; Chu, B. *Polymer* **1979**, *20*, 347.
(10) de Gennes, P. G. *Macromolecules* **1976**, *9*, 587, 594.
(11) Daoud, M.; Jannink, G. *J. Phys. (Paris)* **1978**, *39*, 331.
(12) Dubois-Violette, E.; de Gennes, P. G. *Physics* **1967**, *3*, 181.
(13) Akcasu, A. Z.; Gurol, H. *J. Polym. Sci., Polym. Phys. Ed.* **1976**, *14*, 1.
(14) Daoust, H.; Rinfret, M. *Can. J. Chem.* **1954**, *32*, 492. Parent, M.; Rinfret, M. *Ibid.* **1955**, *33*, 971.
(15) Horth, A.; Rinfret, M. *J. Am. Chem. Soc.* **1955**, *77*, 503.
(16) Staudinger, H. "Die hochmolekularen organischen Verbindungen"; Springer-Verlag: Berlin, 1932; p 128.
(17) Kotin, L. Ph.D. Thesis, Harvard University, 1960.
(18) (a) Benmouna, M.; Akcasu, Z. *Macromolecules* **1978**, *11*, 1187. (b) Akcasu, Z.; Benmouna, M. *Ibid.* **1978**, *11*, 1193.
(19) Farnoux, B. *Ann. Phys.* **1976**, *1*, 73.
(20) Daoud, M. Thesis, Université de Paris VI, 1977.
(21) Daoud, M.; Cotton, J. P.; Farnoux, B.; Jannink, G.; Sarma, G.; Benoit, H.; Duplessix, R.; Picot, C.; de Gennes, P. G. *Macromolecules* **1975**, *8*, 804.
(22) Chen, F. C.; Yeh, A.; Chu, B. *J. Chem. Phys.* **1977**, *66*, 1290.
(23) Tsunashima, Y.; Moro, K.; Chu, B.; Liu, T. Y. *Biopolymers* **1978**, *17*, 251.
(24) Akcasu, A. Z.; Benmouna, M.; Han, C. C. *Polymer* **1980**, *21*, 866.
(25) Muthukumar, M.; Freed, K. F. *Macromolecules* **1978**, *11*, 843.
(26) Koppel, D. F. *J. Chem. Phys.* **1972**, *57*, 4814.
(27) Chu, B.; Gulari, E. *Macromolecules* **1979**, *12*, 445.
(28) Akcasu, A. Z.; Han, C. C. *Macromolecules* **1979**, *12*, 276.

Static and Dynamical Properties of Polystyrene in Carbon Tetrachloride. 2. Osmotic Pressure and Radius of Gyration in the Dilute, Intermediate, and Semidilute Regions†

B. Chu,* K. Kubota, M.-J. He, and Y.-H. Lin

Chemistry Department, State University of New York at Stony Brook, Long Island, New York 11794. *Received March 25, 1980*

ABSTRACT: Static properties, in terms of the absolute scattered intensity, osmotic compressibility, and radius of gyration, of polystyrene ($\bar{M}_w \sim 1 \times 10^7$) in carbon tetrachloride have been studied from dilute to semidilute polymer concentrations of 0.117 wt % at 18 and 25 °C over a range of scattering angles by means of light scattering intensity meaurements. The main purpose of this study is to strengthen our observation of the intermediate concentration region and to show that both static and dynamical properties exhibit a unique behavior for polymer coils in the neighborhood of an overlap concentration C_1^* before entanglement points become appreciable. Our light scattering intensity results appear to agree with earlier reports on changes of the slope in heat of mixing and density of polymer solutions undergoing a change from the dilute to the semidilute region when the solvents are marginal. We have preliminary evidence to suggest that this unique behavior in the intermediate concentration region depends upon previous thermodynamic history of the polymer solution.

I. Introduction

In the previous article,[1] we made appropriate references to recent experiments and theories related to polymer solutions. Therefore, only specific references will be quoted here. In this companion article, the main purpose is to confirm the observation of an anomalous region between dilute and semidilute solutions and to provide a very qualitative physical picture on this unanticipated behavior for polymer coils in solution based on our preliminary observation of both the static and dynamical properties of a high molecular weight polymer sample (polystyrene, $\bar{M}_w \sim 1 \times 10^7$) in carbon tetrachloride.

II. Brief Theoretical Background

The static properties, such as radius of gyration and osmotic pressure, which can be measured by means of light scattering intensity studies in dilute and semidilute solutions have been discussed in detail elsewhere.[2]

(1) Osmotic Pressure. The osmotic compressibility has the form

$$(\partial\pi/\partial C)_{T,P} = H(\partial n/\partial C)^2_{T,P}CRT/R_c(0) \qquad (1)$$

where $R_c(0)$ [$\equiv R_{vv}(0)$] is the excess Rayleigh ratio due to concentration fluctuations obtained from absolute excess scattered intensity extrapolated to zero scattering angle, using vertically polarized incident and scattered light, $H = 4\pi^2 n^2/N_A\lambda_0^4$, and n, C, N_A, T, P, and R are the refractive index of the solution, the polymer concentration in g/cm^3, Avogadro's number, the absolute temperature, the pressure, and the gas constant, respectively.

For dilute polymer solutions, the chemical potential of the solvent, which is denoted by a subscript 1, is related to the osmotic pressure π by

$$(\mu_1 - \mu_1^\circ) = -\pi V_1 \qquad (2)$$

where V_1 is the partial molar volume of the solvent and $\Delta\mu_1$ ($\equiv\mu_1 - \mu_1^\circ$) represents the chemical potential difference for the solution as a whole. The chemical potential difference can be split into an ideal and an excess term, $\Delta\mu_1 = \Delta\mu_1^{id} + \Delta\mu_1^{ex}$ such that

$$\Delta\mu_1^{ex} = \Delta H_1 - T\Delta S_1^{ex} \qquad (3)$$

where ΔH_1 is the partial molar enthalpy of dilution and ΔS_1^{id} ($=\Delta\mu_1^{id}$) is the ideal partial molar entropy of dilution. At the Θ temperature, $\Delta\mu_1^{ex} = 0$. We shall examine the concentration dependence of $\Delta\mu_1$ from polymer solution to the semidilute solution.

By using a lattice model, Flory[3,4] derived for dilute solutions the following relation for $\Delta\mu_1$:

$$\Delta\mu_1 = RT[\ln(1 - v_2) + (1 - 1/x)v_2 + X_1 v_2^2] \qquad (4)$$

†Work supported by the National Science Foundation Chemistry/Polymer Program (DMR 801652) and the U.S. Army Research Office.

0024-9297/81/2214-0392$01.25/0